Macedonian Journal of Chemistry and Chemical Engineering, Vol. **42**, No. 1, pp. xx–xx (2023)

MJCCA9 –

ISSN 1857-5552
e-ISSN 1857-5625

Received: May 4, 2023
Accepted: May 15, 2023

DOI: 10.20450/mjcce.2023.2702
Original scientific paper

INFLUENCE OF ELECTRODEPOSITION REGIME AND Sn:Pd RATIOS IN Sn-Pd ELECTROCATALYSTS ON ETHANOL OXIDATION REACTION

Jelena D. Lović[1,*], Nebojša D. Nikolić[1], Predrag M. Živković[2], Silvana B. Dimitrijević[3], Maja Stevanović[4]

[1]*Department of Electrochemistry, Institute of Chemistry, Technology and Metallurgy, University of Belgrade, Njegoševa 12, Belgrade, Serbia*
[2]*Faculty of Technology and Metallurgy, University of Belgrade, Karnegijeva 4, Belgrade, Serbia*
[3]*Mining and Metallurgy Institute, Zeleni bulevar 35, Bor, Serbia*
[4]*Innovation Centre of the Faculty of Technology and Metallurgy, University of Belgrade, Belgrade, Serbia*
[*]jelena.lovic@ihtm.bg.ac.rs; ORCID iD: 0000-0001-5956-8571

A series of bimetallic Sn-Pd catalysts were prepared by a template-free two step electrodeposition method. According to this method, Sn was electrodeposited firstly in potentiostatic or galvanostatic regime on Cu electrodes in the form of dendrites, then Pd was galvanostatically electrodeposited in the second step on the electrode with the electrodeposited Sn dendrites. The produced Sn-Pd electrocatalysts were compared with an electrocatalyst obtained by Pd electrodeposition on a bare Cu electrode. The morphological and elemental analysis of Sn-Pd and Pd electrocatalysts was performed by means of scanning electron microscopy (SEM) and energy-dispersive X-ray spectroscopy (EDS) techniques. The dendrites of various shapes and degree of branching were obtained by Sn deposition depending on electrodeposition regime, while Pd was electrodeposited in a form of compact Pd islands on both Sn dendrites and the Cu electrode. Cyclic voltammetry (CV) was applied for the electrochemical examination of Sn-Pd and Pd catalysts towards the ethanol oxidation reaction (EOR) in the alkaline solution. The electrocatalyst $Sn_{0.6}$-$Pd_{0.4}$ with an atomic ratio of 60 at.% Sn-40 at.% Pd showed higher oxidation efficiency and better tolerance towards intermediate species in EOR than the other examined electrocatalysts . It was shown that the lower fraction of Pd, relative to Sn, was crucial to achieving optimal synergy of Sn with Pd thus contributing to enhanced electrochemical behavior regarding EOR.

Keywords: electrodeposition; tin; palladium; electrocatalyst; electrooxidation

ВЛИЈАНИЕ НА РЕЖИМОТ НА ЕЛЕКТРОДЕПОЗИЦИЈАТА И НА ОДНОСИТЕ НА Sn:Pd ВО Sn-Pd-ЕЛЕКТРОКАТАЛИЗАТОРИТЕ ВРЗ ОКСИДАЦИЈАТА НА ЕТАНОЛОТ

Серија на биметални катализатори со различни односи на Sn:Pd беа подготвени со методот на двостепена електродепозиција без користење шаблонски протокол. Според овој метод, прво Sn во форма на дендрити беше нанесен електрохемиски во потенциостатски или галваностатски режим врз површината на Cu-електроди. Потоа, во вториот чекор, Pd беше галваностатски нанесен на електродата врз нанесените дендрити од Sn. Вака добиените Sn:Pd-електрокатализатори беа споредени со електрокатализатори добиени со нанесување на Pd на чиста Cu електрода. Морфолошката и елементарната анализа на Sn:Pd и Pd-електрокатализаторите беше направена со помош на скенирачка електронска микроскопија (SEM) и со примена на рендгенска спектроскопија со енергетска дисперзија (EDS). Дендритите со различни форми и различен степен на разгранување беа добиени со нанесување Sn во зависност од режимот на електродепозиција, додека Pd беше нанесен во форма на компактни острови врз дендритите од Pd и Sn на површината на Cu-електродата. Цикличната волтаметрија (CV) беше применета за електрохемиското испитување на Sn:Pd и Pd-катализаторите во од аспект на оксидацијата на етанолот во алкална

средина. Електрокатализаторот $Sn_{0.6}$-$Pd_{0,4}$ со атомски однос од 60 % Sn и 40 % Pd покажа поголема ефикасност на оксидација и поголема толеранција во однос на интермедијарните супстрати отколку другите испитани електрокатализатори. Се покажа дека помал удел на Pd во однос на Sn е еден од клучните фактори за обезбедување оптимална синергија на Sn со Pd, при што на овој начин беше забележана зголемена електрохемиска активност односно оксидацијата на етанолот.

Клучни зборови: електродепозиција; калај; паладиум; електрокатализатори; електрооксидација

1. INTRODUCTION

The synthesis of bimetallic catalysts is one of the most widely investigated topics in materials science.[1–4] The obtained catalysts are playing a leading role in the development of green sources of energy in fuel cells[5,6], batteries[7], sensors[8], organic synthesis[9], photocatalysis[10], and other applications. The commercialization of green sources is obstructed by the high costs, relatively slow electron transfer kinetics, and low stability of the conventional platinum catalysts.[2] Considerable efforts have recently been made to develop new catalytic materials with low costs and high electrochemical activities, durability, and poison resistance for alcohols as sustainable sources of alternative energy. Currently, many studies have focused on Pd-based electrocatalysts for various energy-related reactions. In a comprehensive study of ethanol oxidation reactions (EOR) wherein different catalysts were used, enhancements were founded for Pd-based catalysts modified with tin. Some of the reported catalysts are: atomically ordered intermetallic Pd-Sn composed of an interconnected nanowire network structure[11], carbon supported materials, such as PdSn/C[12–16], carbon nanofiber-supported PdSn/CNFs[17], carbon nanotube-supported PdSn[18], and graphene oxide as support for $Pd_1Sn_{0.4}/TiO_2$-GO catalyst, which exhibited catalytic activity for EOR more than 7 times higher in regard to commercial PdSn/C (JM).[19]

Synthetic methods for the preparation of Pd-based electrocatalysts are numerous, among them is electrochemical deposition.[2,5,20] This is an efficient method of electrocatalyst production since general disadvantages, such as the utilization of expensive organic precursors, the time of synthesis on the high temperatures, and cleaning protocols, are omitted. Electrochemical deposition offers unlimited possibilities to obtain electrocatalysts of varying shapes and composition.[21] When Ni was placed under Pd, the activities of such PdNi catalysts in EOR decreased with respect to the pure Pd catalysts.[22] Unlike Ni, it was shown that Sn as a sub-layer to Pd increases the activity towards EOR.[23–26] Nevertheless, electrodeposition provides the opportunity to develop innovative structure as was shown in our previous investigations.[27,28] Various structures, such as dendrites, needles, and other disperse (irregular) forms, are very desirable for electrocatalytic reactions due to their reasonably large surface area. Ding *et al.* reported Pd–Sn alloy nanocrystals in dendrites with plenty of interface areas and high electroactive sites for EOR.[29] Due to the thin nanosheet structures in Pd-Sn nanodendrites, fast electron transfer and high utilization rate of electrocatalyst in EOR can be achieved. Huang *et al.* prepared PdSn alloy octopods with precisely controlled branches by a simple seed-mediated method.[30] The PdSn octopod-like catalysts exhibited enhanced catalytic activity and stability towards the EOR with respect to commercial Pd/C by more than 6 times.

In our previous work, it was shown that the surface morphology of Sn, as the sub-layer in Sn-Pd electrocatalysts, strongly affects the electrocatalytic activity of Sn-Pd electrocatalysts with a constant atomic ratio of 60 at.% Sn-40 at.% Pd in EOR.[23] The role of Sn was to contribute Pd to oxidize chemisorbed species formed during the electrooxidation of ethanol by providing adsorbed OH^- species[14,15], thereby enhancing the catalytic performance of the bimetallic catalysts. X-ray photoelectron spectroscopy (XPS) measurements showed that the presence of Sn affects the electronic state of Pd by reducing the adsorption strength of the reaction intermediates on Pd, which has a positive effect on Sn-Pd electrocatalytic activity during the EOR.[23] However, the enhancement of the electrocatalyst activity requires adjustment of morphology, as well as optimization of composition.[31,32]

This paper aims to compare Sn-Pd electrocatalysts fabricated by applying constant (both potentiostatic and galvanostatic) regimes for an electrodeposition of Sn dendrites as sub-layers. For further comparison, the Pd electrocatalyst obtained by the electrodeposition method without previous Sn electrodeposition was synthesized. The Sn-Pd electrocatalysts with various atomic ratios of Sn and Pd were also the subject of this

investigation. The electrocatalytic activity of the synthesized electrocatalysts was examined in EOR.

2. EXPERIMENTAL

Cylindrical electrodes of Cu, with a surface area of 0.25 cm^2, were used as a substrate for Sn and Pd electrodeposition. A Cu working electrode was prepared as described previously.[23] All experiments were performed in three-compartment electrochemical glass cells with a Pt electrode as the counter and Ag/AgCl/3.5 M KCl (in the further text, this electrode is denoted as Ag/AgCl) as the reference electrodes. The electrolytes were prepared with high purity water (Millipore, 18 MΩ cm resistivity), and the chemicals were provided by Merck. The experiments were conducted at 298 ± 0.5 K. A BioLogic SP 200 potentiostat/galvanostat was employed.

The Sn-Pd electrocatalysts were synthesized in the following way: in the first step, the Sn electrode, in the form of dendrites, was formed by electrodeposition of Sn on Cu electrodes from de-aerated solution containing 20 g/l $SnCl_2 \times 2H_2O$ in 250 g/l NaOH at a cathodic potential of –1800 mV vs. Ag/AgCl or at a current density of –3 mA cm^{-2}. After the finished electrodeposition process, the formed Sn electrodes were rinsed and transferred to the electrochemical cell containing de-aerated 1 M NH_4Cl and 0.01 M $PdCl_2$. The electrodeposition of Pd (the second step) was performed galvanostatically at a current density of –5 mA cm^{-2}.[33] The electrodes obtained by electrodeposition of Sn at –3 mA cm^{-2} or at –1800 mV vs. Ag/AgCl with 400 mC and Pd electrodeposited galvanostatically with 267 mC were denoted as $Sn_{(-3\ mA\ cm^{-2})}$-Pd and $Sn_{(-1800\ mV)}$-Pd, respectively. In such a way, the bimetallic composition with an atomic ratio of 60 at.% Sn-40 at.% Pd was accomplished. For the sake of comparison, Pd was electrodeposited on Cu using the same electrochemical procedure with the amount of electricity corresponding to that of the bimetallic electrode.

The next set of electrodes was obtained by varying the ratios of Sn and Pd in the Sn-Pd electrocatalysts. In this set, Sn was electrodeposited at –1800 mV vs. Ag/AgCl with 200, 400, 600, and 900 mC, while the amount of electricity for Pd electrodeposition at –5 mA cm^{-2} was kept constant (600 mC). The Sn-Pd electrocatalysts with the following Sn:Pd atomic ratios, 0.25:0.75, 0.4:0.6, 0.5:0.5, and 0.6:0.4, are obtained in this way, and they are denoted as $Sn_{0.25}$-$Pd_{0.75}$, $Sn_{0.4}$-$Pd_{0.6}$, $Sn_{0.5}$-$Pd_{0.5}$, and $Sn_{0.6}$-$Pd_{0.4}$.

After preparation, the electrocatalysts were rinsed with water and transferred into a cell containing 1 M NaOH with 1 M ethanol. EOR were examined using CV by scanning the potential starting from –800 to 200 mV at a rate of 50 mV s^{-1} or by varying the scan rate from 2 mV s^{-1} to 200 mV s^{-1}. In chronoamperometric measurements, the potential was stepped from –800 to –400 mV. The reaction currents obtained in electrochemical experiments were normalized to the mass amount of Pd metal in the catalysts.

The morphology and elemental analysis of Sn, Pd, and Sn-Pd deposits obtained by various electrochemical deposition processes were characterized by scanning electron microscopy (SEM). The following models were used: JEOL JSM-6610LV and JEOL JSM-IT300LV, and both models were equipped with an energy-dispersive X-ray spectrometer (EDS) (Oxford Instruments INCA) attached to the scanning electron microscope and Aztec software.

3. RESULTS AND DISCUSSION

3.1. *Influence of a regime of the electrodeposition*

Figure 1 shows typical morphology and EDS spectrum of Sn electrodeposited galvanostatically on a Cu electrode at a current density of –3 mA cm^{-2} with 400 mC. This current density was 1.5 times larger than the limiting diffusion current density for this alkaline Sn solution.[27] The two dimensional (2D) branchy dendrites (Figs. 1a and 1b) with branches in a form of prisms (Figs. 1c and d) were mostly obtained by electrodeposition at this current density. EDS analysis of the obtained dendrites (Fig. 1e) confirmed a formation of pure Sn by this electrodeposition process.

In the next step, Sn dendrites electrodeposited on a Cu electrode represented the cathode for Pd electrodeposition and the formation of an Sn-Pd electrocatalyst. Pd was electrodeposited galvanostatically at a current density of –5 mA cm^{-2} with 267 mC, whereby the electrocatalyst with an atomic ratio of 60 at.% Sn–40 at.% Pd was obtained. The morphology and the EDS spectrum of the produced Sn-Pd electrocatalyst is shown in Figure 2.

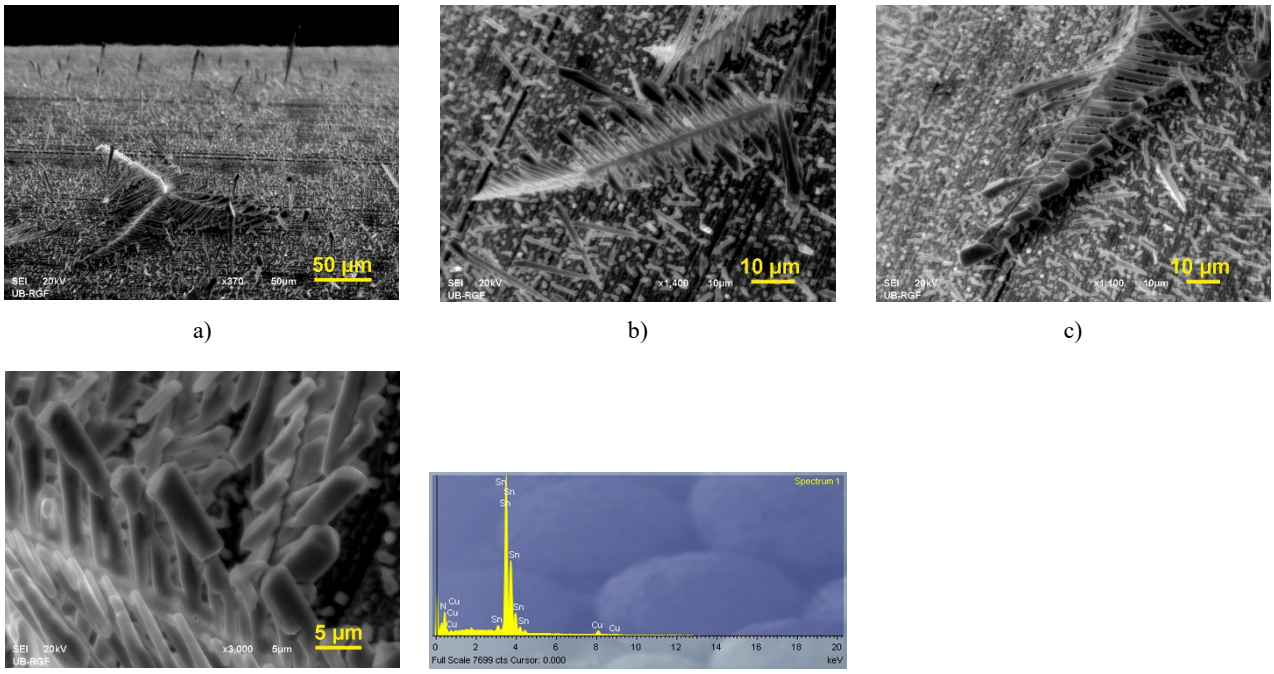

a) b) c)

d) e)

Fig. 1. The morphology and energy-dispersive X-ray spectrum (EDS) of Sn dendrites electrodeposited galvanostatically at a current density of –3 mA cm^{-2} from a solution containing 20 g/l $SnCl_2 \cdot 2H_2O$ in 250 g/l NaOH: **a)** and **b)** macro-morphology, **c)** and **d)** prismatic branches of the dendrites, and **e)** EDS spectrum

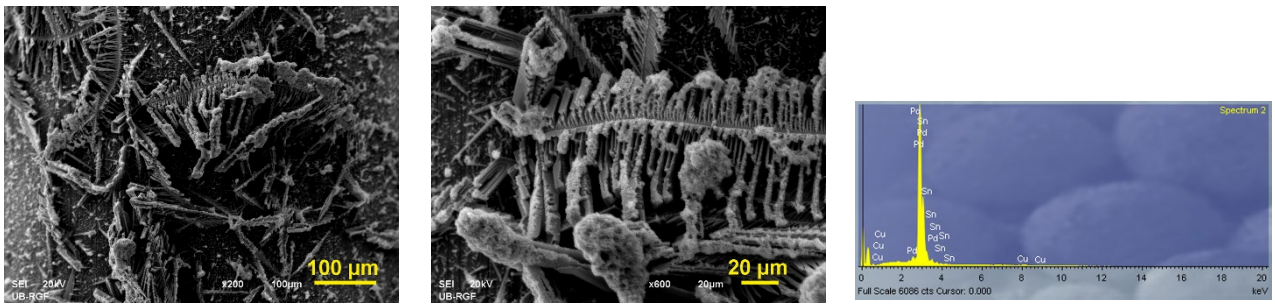

a) b) c)

Fig. 2. The morphology and EDS spectrum of the Sn-Pd electrocatalyst: **a)** and **b)** macro-morphology and **c)** EDS spectrum. Pd was electrodeposited galvanostatically at a current density of –5 mA cm^{-2} on previously galvanostatically synthetized Sn dendrites.

It is obvious from Figure 2a and 2b that a partial coverage of Sn dendrites was achieved by Pd electrodeposition. The main reason for this is the current density distribution effect[23], rather than a lower amount of the electricity used for Pd electrodeposition than that used for Sn electrodeposition. Namely, as a consequence of the current density distribution at the growing surface area, current lines are primarily concentrated at the higher parts of the electrode surface area, causing a preferential electrodeposition and growth of Pd on Sn dendrites relative to the rest of the electrode surface. Electrodeposition of Pd on Sn dendrites was confirmed by EDS analysis (Fig. 2c).

The chronopotentiometry analysis performed at a current density of –3 mA cm^{-2} showed that the largest part of the electrochemical deposition process at this current density corresponded to the chronopotentiometry response from about –1800 mV vs. Ag/AgCl.[28] Following this fact, the galvanostatically produced electrocatalyst is compared with that obtained by a potentiostatic electrodeposition of Sn as a sub-layer on a Cu electrode at a cathodic potential of –1800 mV vs. Ag/AgCl with 400 mC. Electrodeposition of Pd was performed under the same conditions as for the galvanostatically synthesized electrocatalyst (j = –5 mA cm^{-2}; Q = 267 mC), whereby an atomic ratio of 60 at.% Sn-40 at.% Pd was kept.

Figure 3 shows the morphology and EDS spectrum of Sn electrodeposited on a Cu electrode at a cathodic potential of –1800 mV vs. Ag/AgCl with 400 mC.

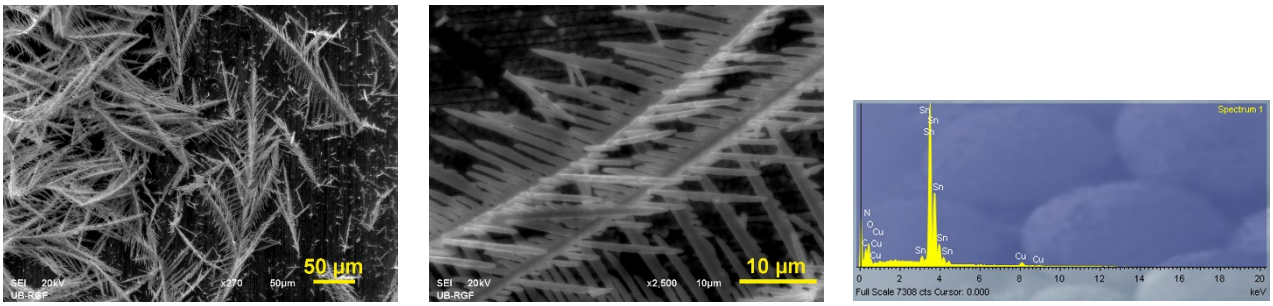

a) b) c)

Fig. 3. The morphology and EDS spectrum of Sn dendrites electrodeposited potentiostatically at a cathodic potential of –1800 mV vs. Ag/AgCl from a solution containing 20 g/l $SnCl_2 \cdot 2H_2O$ in 250 g/l NaOH: **a)** macro morphology, **b)** branches of the dendrites, and **c)** EDS spectrum

The intertwined network of highly-branched fern-like dendrites was obtained. Morphology of the dendrites differed from those obtained galvanostatically. Some of them had the stem-like shape (Fig. 3a). The very tiny branches were obtained under these conditions of electrodeposition (Fig. 3b). Analysis of EDS spectrum (Fig. 3c) confirms the formation of pure Sn.

The morphology and EDS spectrum obtained by Pd electrodeposition at a current density of –5 mA cm^{-2} on the potentiostatically electrodeposited Sn dendrites with 267 mC are shown in Figure 4.

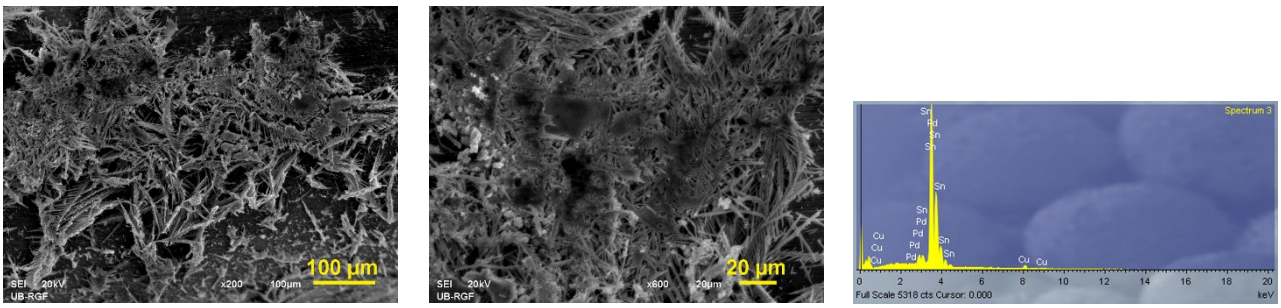

a) b) c)

Fig. 4. The morphology and EDS spectrum of the Sn-Pd electrocatalyst: **a)** and **b)** macro morphology and **c)** EDS spectrum. Pd was electrodeposited galvanostatically at a current density of –5 mA cm^{-2} on previously potentiostatically synthetized Sn dendrites

The partial coverage of Sn dendrites by electrodeposited Pd was also obtained for this electrocatalyst. The compact Pd islands are easy noticeable from Figure 4b. EDS analysis confirmed electrodeposition of Pd on Sn (Fig. 4c).
The synthetized bimetallic electrocatalysts with the corresponding morphologies (Figs. 2 and 4) are denoted as $Sn_{(-3\ mA\ cm^{-2})}$-Pd and $Sn_{(-1800\ mV)}$-Pd, respectively. The electrocatalytic performances of these bimetallic catalysts were evaluated by electrooxidation of ethanol. Typical CVs for EOR on $Sn_{(-3\ mA\ cm^{-2})}$-Pd and $Sn_{(-1800\ mV)}$-Pd are shown in Figure 5. Ethanol electrooxidation exhibited two well-defined current peaks, with the first at ~ –200 mV on the forward scan and the second at ~ –400 mV on the reverse scan. The explanation of this behavior is the following: carbonaceous species formed from ethanol adsorption on the catalyst surface were oxidized in the presence of adsorbed OH^- species, resulting in the current increase until Pd oxide (inactive for EOR) is formed. This leads to a current peak in the forward scan.[33–35] In the reverse scan, the increase of EOR current coincides with a reduction of Pd oxide when Pd sites are being released and active. The current maximum in the reverse scan is due to an oxidation of the carbonaceous species that are not completely oxidized in the forward scan.[35] According to Figure 5, the lower activity of $Sn_{(-3\ mA\ cm^{-2})}$-Pd catalyst with the galvanostatically obtained Sn, compared to the $Sn_{(-1800}$

$_{mV)}$-Pd catalyst with the potentiostatically prepared Sn, can be explained due to lower utilization of Pd on the dendrites with the branches of prismatic shape (Fig. 1) compared to the intertwined network of highly-branched fern-like dendrites (Fig. 3). It can be rationalized that morphological properties of Sn contribute and determine Pd's electrochemical behavior in EOR.

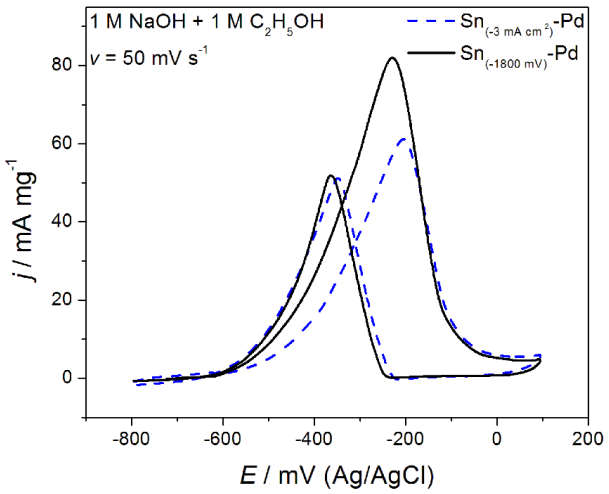

Fig. 5. Cyclic voltammograms (CVs) of $Sn_{(-3\ mA\ cm^{-2})}$-Pd and $Sn_{(-1800\ mV)}$-Pd electrocatalysts in 1 M NaOH + 1 M C_2H_5OH solution recorded at v = 50 mV s^{-1}

The lower initial potential (E_{in}), as well as the lower peak potential (E_p), signify that the electrocatalyst is more favorable for use in EOR and exhibits better tolerance towards the intermediate species.[18] The carbonaceous intermediated species can be well removed from the catalyst surface, which results in reactivation of the Pd active sites. It is found that the $Sn_{(-1800\ mV)}$-Pd catalyst has the more negative E_{in} and E_p values by approximately 30 mV compared to $Sn_{(-3\ mA\ cm^{-2})}$-Pd, signifying higher oxidation efficiency for EOR. It seems that adsorbed OH^- species are more easily formed on the $Sn_{(-1800\ mV)}$-Pd catalyst due to more branchy Sn dendrite morphology.

Since Sn has no catalytic activity in the potential range of EOR[23], the electrooxidation of ethanol on the Sn-Pd catalysts is mainly attributed to the electrocatalysis of the Pd component. Consequently, Pd as the main catalyst was further analyzed. Figure 6 shows the morphology (Fig. 6a and b) and the EDS spectrum (Fig. 6c) of Pd obtained by galvanostatic electrodeposition on a Cu electrode at a current density of –5 mA cm^{-2} with 267 mC. The partial coverage of a Cu electrode by electrodeposited Pd islands is clearly visible from Figures 6a and 6b. Electrodeposition of Pd on Cu was confirmed by EDS analysis (Fig. 6c).

The electrochemical behavior of Pd electrodeposited on Cu in the EOR is shown in Figure 7. The shape of CV of EOR obtained for electrodeposition of Pd on Cu differs in respect to the one acquired for the EOR on polycrystalline Pd.[36] Therefore, the electrochemical response of Pd in EOR was strongly influenced by Cu substrate as a catalyst support.[23]

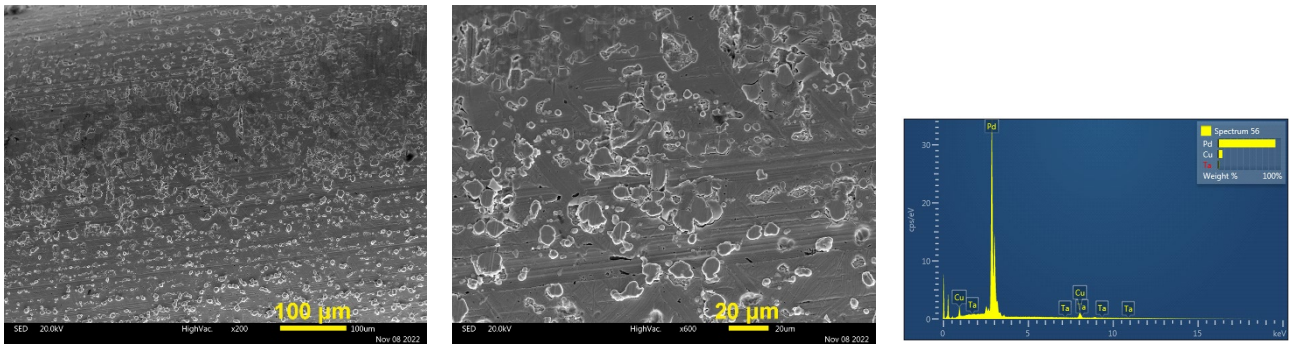

a) b) c)

Fig. 6. The morphology and EDS spectrum of Pd electrodeposited galvanostatically at a current density of –5 mA cm^{-2} from 1 M NH_4Cl and 0.01 M $PdCl_2$: **a)** and **b)** macro-morphology and **c)** EDS spectrum

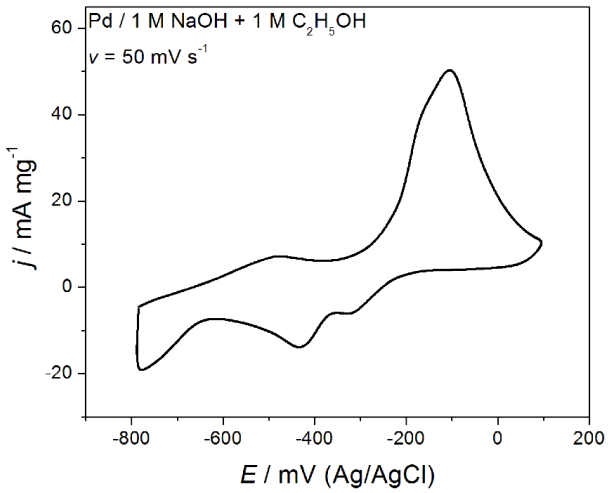

Fig. 7. CV of a Pd electrocatalyst in 1 M NaOH + 1 M C_2H_5OH solution recorded at $v = 50$ mV s^{-1}

Cyclic voltammetry is the most extensively used technique for achieving qualitative data about electrochemical reactions.[17,18,34,37] Aside from the CV technique, square wave voltammetry is an often-used technique for kinetics and analytical investigations due to the improved voltametric characteristics compared to CV.[38] Certainly, since the current peaks for EOR are well expressed (Figs. 5 and 7), EOR was investigated by CV in terms of mass transport properties. The influence of various potential scan rates on the electrochemical behavior of the Pd (Fig. 8a) and $Sn_{(-1800\ mV)}$-Pd (Fig. 8b) electrocatalysts in EOR was examined. According to Figure 8, an increase in the current density of forward peaks is shown with an increase in scan rate for both investigated electrodes. Moreover, the forward peak potential is shifted in the positive direction. Linear dependency of the peak current density versus the square root of the scan rate was observed for the potential scan rates from 2 to 200 mV s^{-1}, while for $v > 200$ mV s^{-1}, deviation from linearity was noticed. Therefore, linear dependency j_p *vs.* $v^{0.5}$ confirmed that the EOR on the Pd and $Sn_{(-1800\ mV)}$-Pd electrocatalysts was controlled by the diffusion process.[17,33]

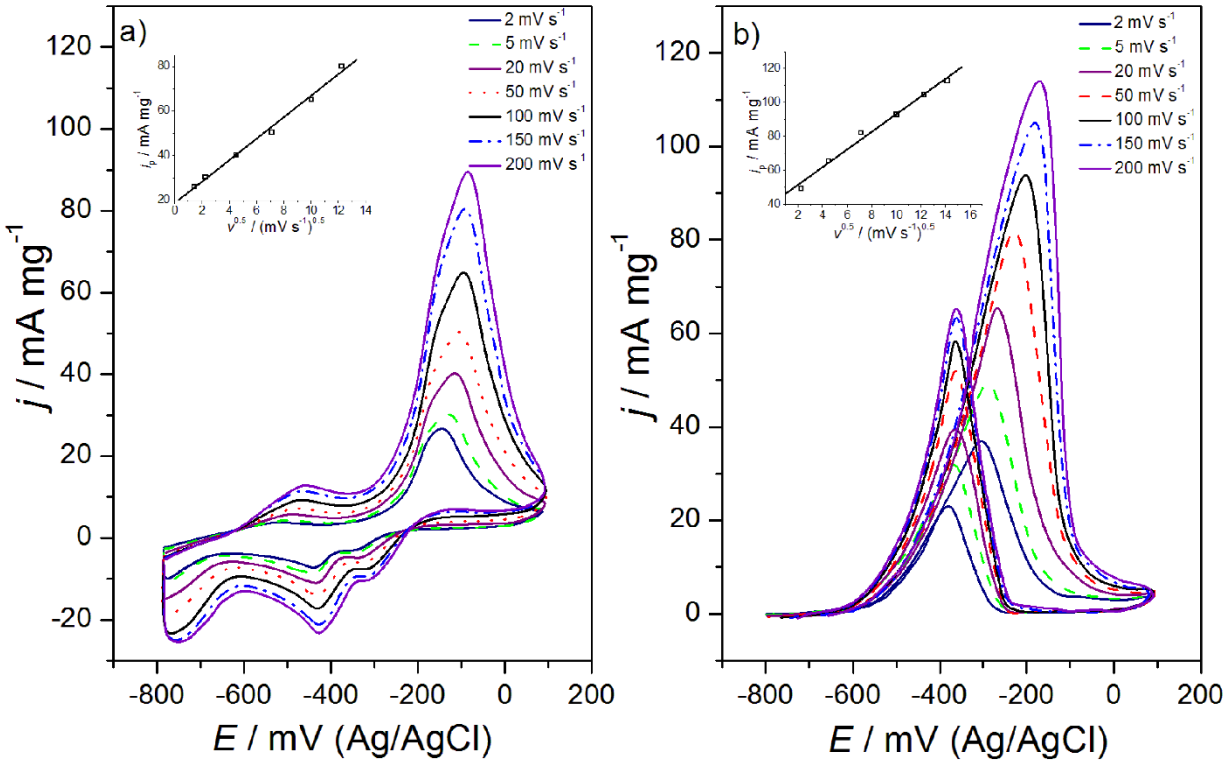

Fig. 8. CVs of (a) Pd and (b) $Sn_{(-1800\ mV)}$-Pd electrocatalysts in 1 M NaOH + 1 M C_2H_5OH solution recorded at $v = 2$, 5, 20, 50, 100, 150, and 200 mV s^{-1}. Inset: dependency of j_p from $v^{0.5}$

A further examination of Sn-Pd electrocatalysts on electrocatalytic activity in ethanol oxidation was performed through analysis of various atomic ratios of Sn and Pd in electrocatalysts produced with potentiostatically electrodeposited Sn at –1800 mV vs. Ag/AgCl as the sub-layer. Varios atomic ratios of Sn and Pd were attained by varying of the amount of the

electricity used for Sn electrodeposition. Since during a potentiostatic regime of the electrodeposition the real current density remains constant,[21] the morphology of electrodeposited metals is only dependent on a cathodic potential applied for an electrodeposition process not on the amount of the passed electricity. For that reason, additional morphological analysis of Sn and Sn-Pd electrocatalysts was not performed.

3.2. *Effect of Sn deposited charge for constant potential*

Figure 9 illustrates CVs for EOR on Sn-Pd electrocatalysts with constant Pd loading versus different amounts of Sn loading. The purpose of this part was to find out the optimum amount of Sn which accomplished the highest electrocatalytic activity towards EOR among various Sn-Pd electrocatalysts. The following Sn-Pd ratios were analyzed: 0.25:0.75, 0.4:0.6, 0.5:0.5, and 0.6:0.4. In the forward scan, the current densities reach a maximum at –0.23 V for $Sn_{0.6}$-$Pd_{0.4}$ and $Sn_{0.5}$-$Pd_{0.5}$ and at –0.19 V for $Sn_{0.4}$-$Pd_{0.6}$ and $Sn_{0.25}$-$Pd_{0.75}$ electrocatalysts. Among the CVs of the investigated Sn-Pd catalysts for the EOR, the most active one was found to be $Sn_{0.6}$-$Pd_{0.4}$, with the current densities of the forward peak being 1.3, 1.75, and 2.6 times higher than those for $Sn_{0.5}$-$Pd_{0.5}$, $Sn_{0.4}$-$Pd_{0.6}$, and $Sn_{0.25}$-$Pd_{0.75}$, respectively (Fig. 9).

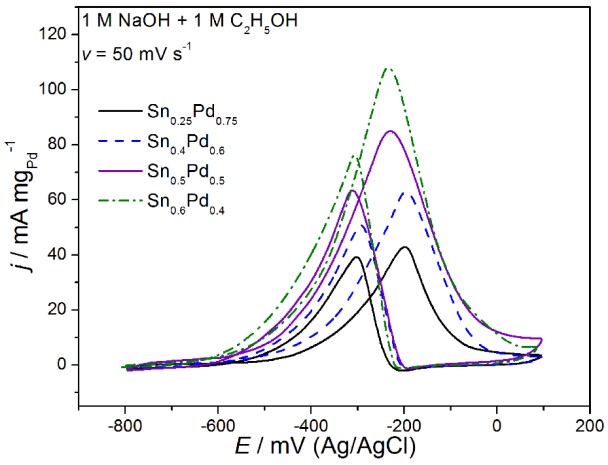

Fig. 9. CVs of $Sn_{0.25}$-$Pd_{0.75}$, $Sn_{0.4}$-$Pd_{0.6}$, $Sn_{0.5}$-$Pd_{0.5}$, and $Sn_{0.6}$-$Pd_{0.4}$ electrocatalysts in 1 M NaOH + 1 M C_2H_5OH solution recorded at v = 50 mV s^{-1}

The ratio of j_f (the peaking current density of the forward scan)/j_b (the peaking current density of the backward scan) is applied to evaluate the anti-poisoning ability of catalysts.[18] The obtained values of j_f/j_b are 1.10, 1.20, 1.28, and 1.50 for $Sn_{0.25}$-$Pd_{0.75}$, $Sn_{0.4}$-$Pd_{0.6}$, $Sn_{0.5}$-$Pd_{0.5}$, and $Sn_{0.6}$-$Pd_{0.4}$, respectively, as illustrated in Figure 10. Therefore, $Sn_{0.6}$-$Pd_{0.4}$ exhibited the highest anti-poisoning ability. The excellent electrochemical activity of the $Sn_{0.6}$-$Pd_{0.4}$ catalyst should be derived from the bi-functional mechanism of the Sn-Pd catalyst and the presence of Sn, which absorb OH^- and participate in the removal of the carbonaceous species produced during the oxidation of ethanol and timely release of the active sites of Pd, leading to the enhancement of the overall ethanol oxidation kinetics. The established electrochemical performances of $Sn_{0.6}$-$Pd_{0.4}$ can be rationalized over the optimum amount of Sn and Pd, which provide better utilization of Pd as illustrated in Figure 9.

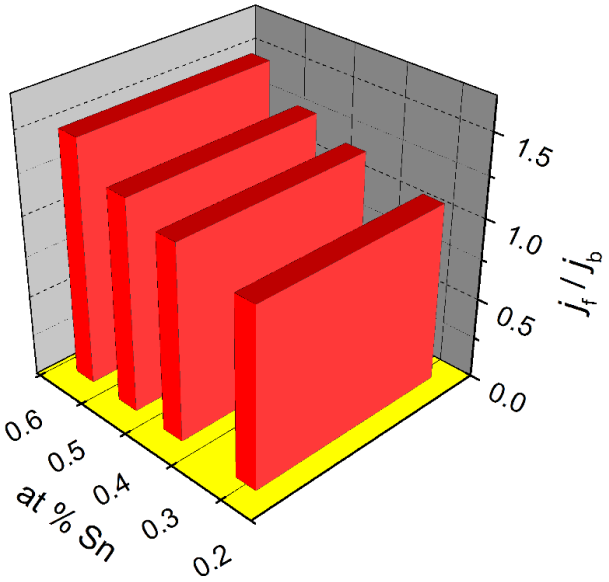

Fig. 10. Dependencies of j_f/j_b from the fraction of Sn in Sn-Pd catalysts (data derived from Fig. 9)

4. CONCLUSIONS

This work investigated the bimetallic Sn-Pd electrocatalysts synthesized by means of a two-step template-free electrodeposition method and their electrocatalytic activity in EOR. A comparison was made with an electrolytically produced Pd electrocatalyst. Depending on the electrodeposition conditions, various forms of Sn dendrites were obtained. Subsequently, Sn was used as a sub-layer for Pd electrodeposition, and it was shown that Pd partially covered Sn. Concerning electrocatalytic behavior, it was determined that different morphological characteristics of Sn contribute to and affect Pd electrochemical behavior in EOR. Examination of mass transport properties revealed that the EOR are the diffusion-controlled processes on Sn-Pd

and Pd electrocatalysts. By varying the amount of Sn loading prepared in the potentiostatic regime and keeping a constant Pd loading, a series of Sn-Pd electrocatalysts with various ratios of Sn and Pd were synthesized, and among them, $Sn_{0.6}$-$Pd_{0.4}$ was determined to be the most active and poison-tolerant catalyst in EOR. It was pointed out that optimization of composition and morphology assures well synergy of Sn with Pd towards EOR. Based on the presented results, better electrochemical properties can be fulfilled with a lower fraction of Pd compared to Sn, which also reduces the cost of bimetallic Sn-Pd catalysts and opens new perspectives for possible practical applications.

Acknowledgments: This work was funded by the Ministry of Science, Technological Development and Innovation of the Republic of Serbia (RS) (Grant No. 451-03-47/2023-01/200026) and the Science Fund of RS (Grant No. AdCatFC: 7739802).

REFERENCES

(1) Halim, E. M.; Chemchoub, S.; El Attar, A.; Salih, F. E.; Oularbi, L.; El Rhazi, M., Recent advances in anode metallic catalysts supported on conducting polymer-based materials for direct alcohol fuel cells. *Front. Energy Res*. **2022,** *10*, 843736. https://doi.org/10.3389/fenrg.2022.843736

(2) Serov, A.; Kwak, C., Review of non-platinum anode catalysts for DMFC and PEMFC application. *Appl. Catal. B – Environ.* **2009**, *90*, 313–320. https://doi.org/10.1016/j.apcatb.2009.03.030

(3) Wang, K. W.; Kang, W. D.; Wei, Y. C.; Liu, C. W.; Su, P. C.; Chen, H. S.; Chung, S. R., Promotion of PdCu/C catalysts for ethanol oxidation in alkaline solution by SnO_2 modifier. *Chemcatchem* **2012**, *4*, 1154 – 1161. https://doi.org/10.1002/cctc.201100500

(4) Guo, J.; Jiao, S.; Ya, X.; Zheng, H.; Wang, R.; Jiao Yu, J.; Wang, H.; Zhang, Z.; Liu, W.; He, C.; Fu, X. Ultrathin Pd-based perforated nanosheets for fuel cells electrocatalysis. *Chemelectrochem* **2022**, *9*, 202200729. https://doi.org/10.1002/celc.202200729

(5) Elsaid, K.; Abdelfatah, S.; Abdel Elabsir, A. M.; Hassiba, R. J.; Ghouri, Z. K.; Vechot, L., Direct alcohol fuel cells: Assessment of the fuel's safety and health aspects. *Int. J. Hydrogen Energ*. **2021**, *46*, 30658–30668. https://doi.org/10.1016/j.ijhydene.2020.12.009

(6) Bianchini, C.; Shen, P. K., Palladium-based electrocatalysts for alcohol oxidation in half cells and in direct alcohol fuel cells. *Chem. Rev.* **2009,** *109,* 4183–4206. https://doi.org/10.1021/cr9000995

(7) Chiu, H.; Brodusch, N.; Gauvin, R.; Guerfi, A.; Zaghib, K., Demopoulos, G. P., Aqueous synthesized nanostructured $Li_4Ti_5O_{12}$ for high-performance lithium ion battery anodes. *J. Electrochem. Soc.* **2013**, *160*, A3041–A3047. DOI:10.1149/2.008305jes

(8) Singh, S.; Sharma, S., Temperature dependent selective detection of ethanol and methanol using MoS_2/TiO_2 composite. *Sensors Actuat. B – Chem*. **2022**, *350*, 130798. https://doi.org/10.1016/j.snb.2021.130798

(9) Xu, J.; Wilson, A. R.; Rathmell, A. R.; Howe, J.; Chi, M. Wiley, B. J. Synthesis and catalytic properties of Au–Pd nanoflowers. *ACS Nano* **2011**, *5*, 6119–6127. https://doi.org/10.1021/nn201161m

(10) Liang, Y.; Ma, L.; Cui, Z.; Li, Z.; Zhu, S.; Yang, X., Facile in situ hydrothermal method for synthesis of $SrTiO_3/TiO_2$ nanostructures with improved photoelectrochemical activities. *J. Electrochem. Soc.* **2013**, *160*, H704–H709. DOI:10.1149/2.045310jes

(11) Cao, Z.; Lao, X.; Gao, F.; Yang, M.; Sun, J.; Liu, X.; Su, R.; Chen, J.; Guo, P., Improvement of electrocatalytic alcohol oxidation by tuning the phase structure of atomically ordered intermetallic Pd-Sn nanowire networks. *Sci. China Mater.* **2022**, *65(10)*, 2694–2703. https://doi.org/10.1007/s40843-022-2069-8

(12) Fontes, E. H.; Ramos, C. E.; Nandenha, J.; Piasentin, R. M.; Neto, A. O.; Landers, R., Structural analysis of PdRh/C and PdSn/C and its use as electrocatalysts for ethanol oxidation in alkaline medium. *Int. J. Hydrogen Energ*. **2019**, *44,* 937–951. https://doi.org/10.1016/j.ijhydene.2018.11.049

(13) Geraldes, A. N.; Furtunato da Silva, D.; Martins da Silva, J. C.; Antonio de Sa, O.; Spinace, E. V.; Neto, A. O; Dos Santos, M. C., Palladium and palladiumetin supported on multi wall carbon nanotubes or carbon for alkaline direct ethanol fuel cell. *J. Power Sources* **2015**, *275*, 189–199. http://dx.doi.org/10.1016/j.jpowsour.2014.11.024

(14) Du, W.; Mackenzie, K. E.; Milano, D. F.; Deskins, N. A.; Su, D.; Teng, X., Palladium–tin alloyed catalysts for the ethanol oxidation reaction in an alkaline medium. *ACS Catal*. **2012**, *2*, 287–297. https://doi.org/10.1021/cs2005955

(15) Makin Adam, A. M.; Zhu, A.; Ning, L.; Deng, M.; Zhang, Q.; Liu, Q., Carbon supported PdSn nanocatalysts with enhanced performance for ethanol electrooxidation in alkaline medium. *Int. J. Hydrogen Energ*. **2019**, *44*, 20368–20379. https://doi.org/10.1016/j.ijhydene.2019.06.013

(16) Pinheiro, V. S.; Souza, F. M.; Gentil, T. C.; Nascimento, A. N.; Bohnstedt, P.; Parreira, L. S.; Paz, E. C.; Hammer, P.; Sairre, M. I.; Batista, B. L.; Santos, M. C. *Renew. Energ*. **2020**, *158*, 49–63. https://doi.org/10.1016/j.renene.2020.05.050

(17) Selepe, C. T.; Gwebu, S. S.; Matthews, T.; Mashola, T. A.; Sikeyi, L. L.; Zikhali, M.; Mbokazi, S. P.; Makhunga, T. S.; Adegoke, K. A.; Maxakato, N. W., Electro-catalytic properties of palladium and palladium alloy electro-catalysts supported on carbon nanofibers for electro oxidation of methanol and ethanol in alkaline medium. *Catalysts* **2022**, *12*, 608. https://doi.org/10.3390/catal12060608

(18) Ning, L.; Liu, X.; Deng, M.; Huang, Z.; Zhu, A.; Zhang, Q.; Liu, Q., Palladium-based nanocatalysts anchored on CNT with high activity and durability for ethanol electro-oxidation. *Electrochim. Acta* **2019**, *297*, 206–214. https://doi.org/10.1016/j.electacta.2018.11.188

(19) Wang, X.; Zhang, C.; Chi, M.; Wei, M.; Dong, X.; Zhu, A.; Zhang, Q.; Liu, Q., Two-dimensional PdSn/TiO_2-GO

towards ethanol electrooxidation catalyst with high stability. *Int. J. Hydrogen Energ*. **2021**, *44*, 19129–19139. https://doi.org/10.1016/j.ijhydene.2021.03.058

(20) Bliznakov, S.; Vukmirovic, M.; Sutter, E.; Adzic, R., Electrodeposition of Pd nanowires and nanorods on carbon nanoparticles. *Maced. J. Chem. Chem. Eng.* **2011**, *30(1)*, 19–27.

(21) Popov, K. I.; Djokić, S. S.; Nikolić, N. D.; Jović, V. D., *Morphology of Electrochemically and Chemically Deposited Metals*; Springer: New York, NY, USA, **2016**. https://doi.org/10.1007/978-3-319-26073-0

(22) Miao, B.; Wu, Z. P.; Zhang, M.; Chen, Y.; Wang, L. Role of Ni in bimetallic PdNi catalysts for ethanol oxidation reaction. *J. Phys. Chem. C* **2018**, *122*, 22448−22459. https://doi.org/10.1021/acs.jpcc.8b05812

(23) Lović, J. D.; Eraković Pantović, S.; Rakočević, L. Z.; Ignjatović, N. L.; Dimitrijević, S. B.; Nikolić, N. D., A novel two-step electrochemical deposition method for Sn-Pd electrocatalyst synthesis for a potential application in direct ethanol fuel cells. *Processes* **2023**, *11*, 120. https://doi.org/10.3390/pr11010120

(24) Xaba, N.; Modibedi, R. M.; Mathe, M. K.; Khotseng, L. E., Pd, PdSn, PdBi, and PdBiSn nanostructured thin films for the electro-oxidation of ethanol in alkaline media. *Electrocatalysis* **2019**, *10*, 332–341. https://doi.org/10.1007/s12678-019-0511-9

(25) Mavrokefalos, C. K.; Hasan, M.;, Khunsin, W.; Schmidt, M.; Maier, S. A.; Rohan, J. F.; Compton, R. C.; Foord, J. S., Electrochemically modified boron-doped diamond electrode with Pd and Pd-Sn nanoparticles for ethanol electrooxidation. *Electrochim. Acta* **2017**, *243*, 310–319. http://dx.doi.org/10.1016/j.electacta.2017.05.039

(26) Lee, S. H.; Jo, Y. R.; Noh, Y.; Kim, B. J.; Kim, W. B., Fabrication of hierarchically branched SnO_2 nanowires by two-step deposition method and their applications to electrocatalyst support and Li ion electrode. *J. Power Sources* **2017**, *367*, 1–7. http://dx.doi.org/10.1016/j.jpowsour.2017.09.045

(27) Nikolić, N. D.; Lović, J. D.; Maksimović, V. M.; Živković, P. M., Morphology and structure of electrolytically synthesized tin dendritic nano-structures. *Metals* **2022**, *12(7)*, 1201. https://doi.org/10.3390/met12071201

(28) Nikolić, N. D.; Lović, J. D.; Maksimović, V. M. The control of morphology and structure of galvanostatically produced tin dendrites by analysis of chrono-potentiometry response. *J. Solid State Electrochem.* **2023**. https://doi.org/10.1007/s10008-023-05380-6

(29) Ding, L. X.; Wang, A. L.; Ou, Y. N.; Li, Q.; Guo, R.; Zhao, W. X.; Tong,Y. X.; Li, G. R., Hierarchical Pd-Sn alloy nanosheet dendrites: an economical and highly active catalyst for ethanol electrooxidation. *Sci. Rep*. **2013**, *3*, 1181. https://doi.org/10.1038/srep01181

(30) Huang, J.; Ji, L.; Li, X.; Wu, X.; Qian, N.; Li, J.; Yan, Y.; Yang, D.; Zhang, H., Facile synthesis of PdSn alloy octopods through the Stranski–Krastanov growth mechanism as electrocatalysts towards the ethanol oxidation reaction. *Crystengcomm*, **2022**, *24*, 3230. https://doi.org/10.1039/D2CE00242F.

(31) Li, S.; Shu, J.; Ma, S.; Yang, H.; Jin, J.; Zhang, X.; Jin, R., Engineering three-dimensional nitrogen-doped carbon black embedding nitrogen-doped graphene anchoring ultrafine surface-clean Pd nanoparticles as efficient ethanol oxidation electrocatalyst. *Appl. Catal. B* **2021**, *280*, 119464. https://doi.org/10.1016/j.apcatb.2020.119464

(32) Lima, F. H. B.; Profeti, D.; Lizcano-Valbuena, W. H.; Ticianelli, E. A.; Gonzalez, E. R., Carbon-dispersed Pt–Rh nanoparticles for ethanol electro-oxidation. Effect of the crystallite size and of temperature. *J. Electroanal. Chem.* **2008**, *617(2)*, 121–129. https://doi.org/10.1016/j.jelechem.2008.01.024

(33) Lović, J. D.; Jović, V. D., Electrodeposited Pd and PdNi coatings as electrodes for the electrochemical oxidation of ethanol in alkaline media. *J. Solid State Electrochem*. **2017**, *21*, 2433–2441. https://doi.org/10.1007/s10008-017-3595-2

(34) Hasan, M.; Khunsin, W.; Mavrokefalos, C. K.; Maier, S. A.; Rohan, J. F.; Foord, J. S., Facile electrochemical synthesis of Pd nanoparticles with enhanced electrocatalytic properties from surfactant-free electrolyte. *ChemElectroChem* **2018**, *5(4)*, 619–629. https://doi.org/10.1002/celc.201701132

(35) Santos, R. M. I. S.; Nakazato, R. Z.; Ciapina, E. G., The dual role of the surface oxophilicity in the electro-oxidation of ethanol on nanostructured Pd/C in alkaline media. *J. Electroanal. Chem.* **2021**, *894*, 115342. https://doi.org/10.1016/j.jelechem.2021.115342

(36) Liang, Z. X.; Zhao, T. S.; Xu, J. B.; Zhu, L. D., Mechanism study of the ethanol oxidation reaction on palladium in alkaline media. *Electrochim. Acta* **2009**, *54*, 2203–2208. https://doi.org/10.1016/j.electacta.2008.10.034

(37) Gulaboski, R., The future of voltammetry, *Maced. J. Chem. Chem. Eng*. **2022**, *41(2)*, 151–162. https://doi.org/10.20450/mjcce.2022.2555

(38) Gulaboski, R.; Mirčeski, V., Surface catalytic mechanism-theoretical study under conditions of differential square-wave voltammetry, *Maced. J. Chem. Chem. Eng*. **2022**, *41(1)*, 1–10. https://doi.org/10.20450/mjcce.2022.2404